

## MODELING STUDIES ON THE LOW $\beta_y$ LATTICE

**Annick Ropert, ESRF**

### **Introduction**

The N = 40 low  $\beta_y$  lattice (which had not been used since Run 1997-7) was re-commissioned at the beginning of Run 1998-2. The testing of the optics addressed several puzzling questions:

- strong discrepancy of the vertical  $\beta$ -function with respect to the model, thus making it necessary to detune Q1 by more than 6% in order to get closer to theoretical  $\beta$ -functions,
- very small energy acceptance, which is very likely responsible for the moderate lifetime,
- strong dependence of the lifetime on the closed orbit pattern.

These pending questions have triggered the work presently reported in this note. The studies were focused on understanding the discrepancies between the real machine and the model and on deriving an improved modeling for the lattice. The results of  $\beta$ -function measurements were the main input for these studies. In parallel with a review of the main sources of modulation, these data are interpreted and discussed in the following sections.

### **Main results during re-commissioning**

#### *1. Discrepancy between the model and $\beta$ -function measurements*

The same magnet configuration as during former operation of the N = 40 low  $\beta_y$  optics was used (SCR file: SR-1998-061-0302-105314). Figure 1 shows the results of the early  $\beta$ -function measurements performed on Mar 2. Vertical  $\beta$ -functions show a significant discrepancy in the vertical plane with respect to the model, more specially in the achromat. This led to make systematic changes in the Q1 family while keeping the tunes constant by readjusting Q2 and Q3. The final configuration corresponds to an increase of Q1 by 14 A with respect to previous files, i.e., more than 6%. The  $\beta$ -functions were measured in two sectors and in some Q4 quadrupoles. Results are given in Figure 2. For simplicity, measurements in different sectors are superimposed on a single sector graph. The agreement with the model is good in the horizontal plane. In the vertical plane, the  $\beta$  at the B:Q4 location is about 15% lower than expected on the average.

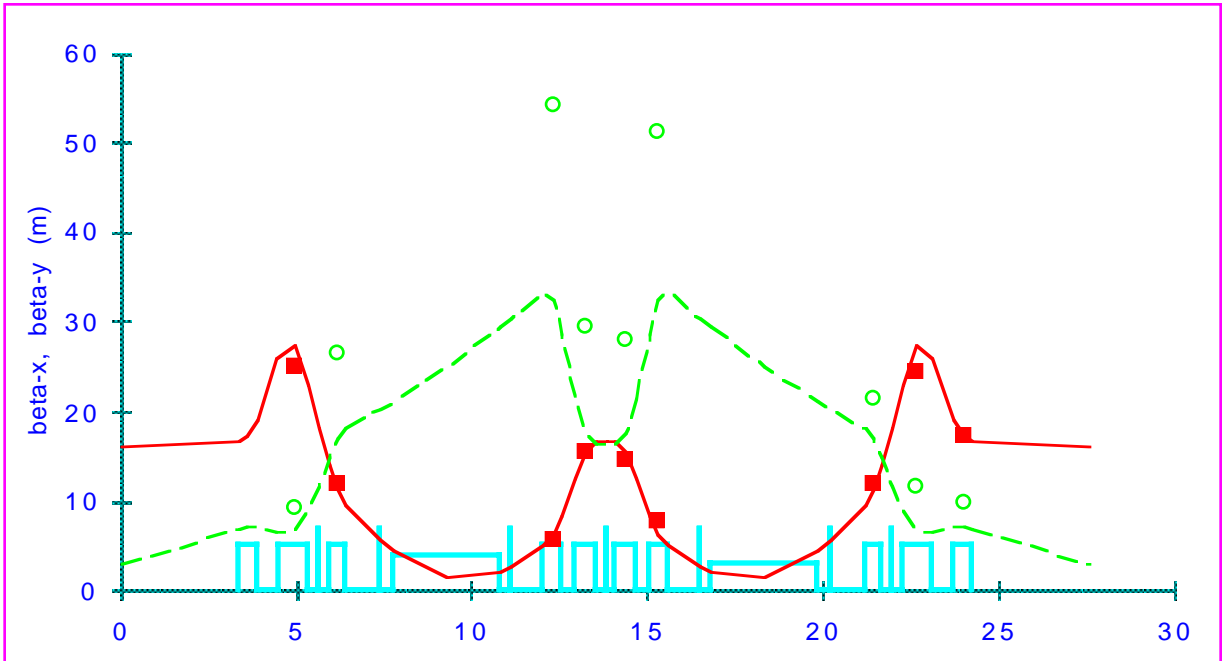


Figure 1.  $\beta$ -function measurements with nominal Q1

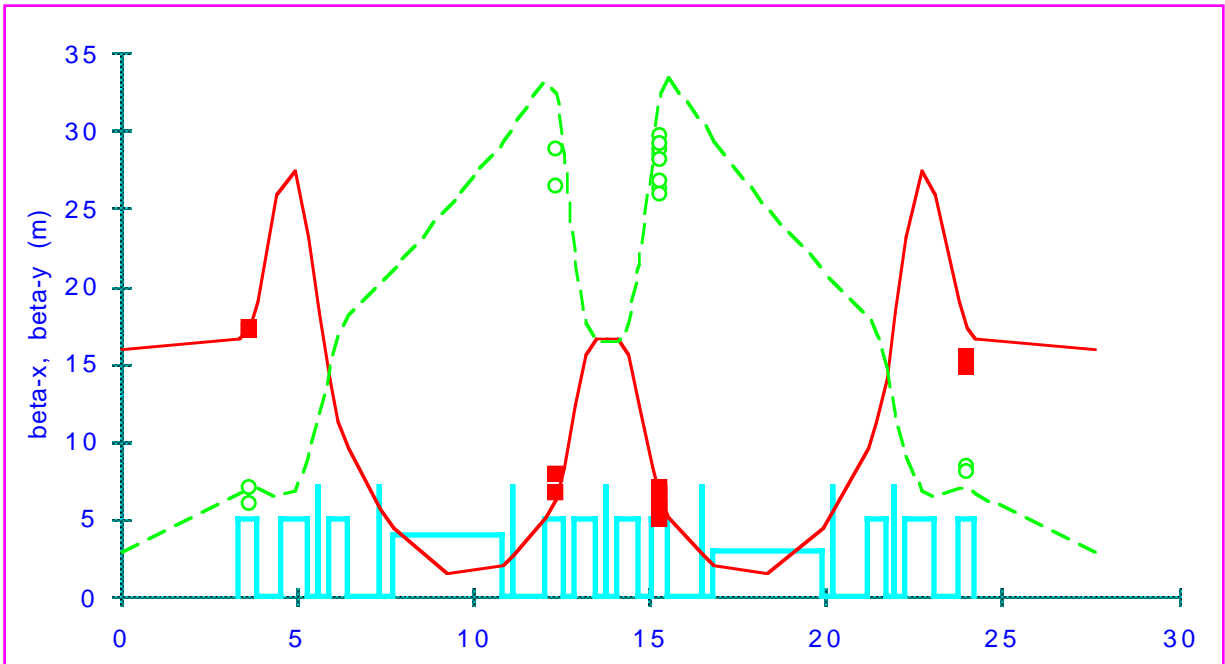


Figure 2.  $\beta$ -function measurements with +14 A on Q1

## 2. Energy acceptance

The energy acceptance was measured using the classical scan in rf frequency. As shown in Figure 3, it is surprisingly small, as compared to October 1997 measurements. Given this puzzling result, the machine was switched back to the low  $\beta_y$  insertion optics in order to get a comparison with the energy acceptance of this optics. Nothing abnormal was found.

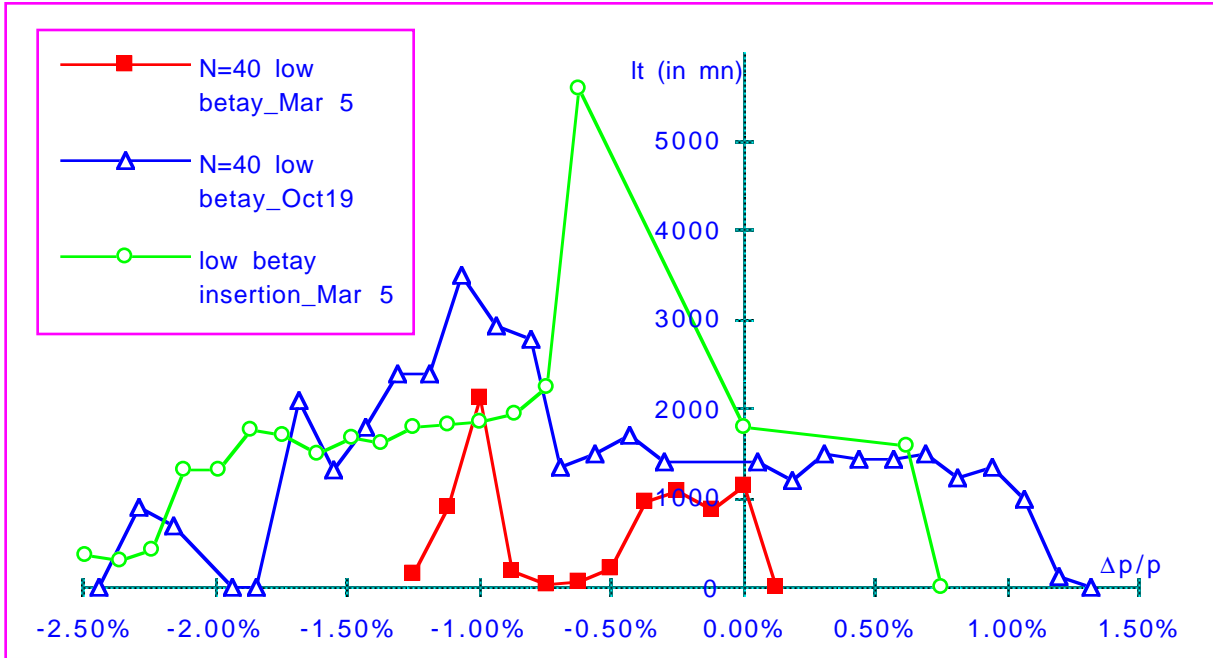


Figure 3. Lifetime evolution as a function of energy deviation

## 3. Lifetime

Lifetime measurements under various conditions are summarized in Table 1 for 100 mA in 6 bunches + 25 triplets. The dependence of the lifetime on the orbit steering is likely due to the additional focusing effects induced by the different off-centered orbits in sextupoles (energy acceptance, excitation of resonances ?). This has to be investigated in detail.

Table 1

	lt (in mn)
low $\beta_y$ insertion	1800
N = 40 low $\beta_y$ with user orbit	500
N= 40 low $\beta_y$ with a "moderately successful" attempt to steer to zero-orbit	650
N = 40 low $\beta_y$ with H correctors from 14.3 low $\beta_y$ user orbit	1300

## **Model and quadrupole calibration**

The low  $\beta_y$  optics tuned at  $\nu_y = 19.3$  is derived from the  $\nu_y = 14.3$  optics by readjusting quadrupoles Q1, Q2, Q3 in the straight sections in order to achieve the desired  $\beta_y = 3$  m at the center of the straight sections and phase advances per cell in both planes ( $\nu_x$  is kept at 35.2). The quadrupoles in the achromats remain unchanged. The present model, which is used to derive quadrupole currents, is based on expected magnetic quadrupole lengths.

Magnet currents are derived from the measured  $I$ ,  $BnL$  data resulting from magnetic measurements (see Figure 4). It has to be noted that the operating conditions of several quadrupoles (Q4, Q5, and Q2 to a lesser extent) correspond to the region of the  $BnL/I = f(I)$  curves where the slope varies rapidly. This can affect the precision of the calibration.

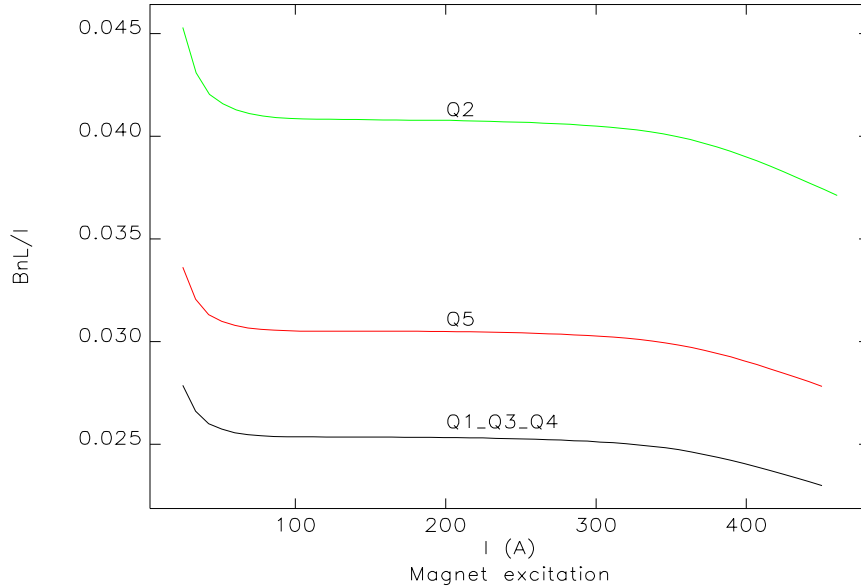


**Figure 4.** Excitation curves for the different types of quadrupoles

In the following, we use the data from a typical quadrupole for each quadrupole family and derive the currents corresponding to the  $KnL$  ( $KnL = BnL * B\rho$ ) values of the model by a linear interpolation. The desired  $BnL$  is associated with the  $n^{th}$  and  $n+1^{th}$  values of the measured tables, and the following interpolation applied:

$$I = I_{meas}(n) + \frac{I_{meas}(n+1) - I_{meas}(n)}{BnL_{meas}(n+1) - BnL_{meas}(n)} [BnL - BnL_{meas}(n)].$$

In the same way, KnL values can be derived from the operating currents by

$$BnL = BnL_{meas}(n) + \frac{BnL_{meas}(n+1) - BnL_{meas}(n)}{I_{meas}(n+1) - I_{meas}(n)} [I - I_{meas}(n)].$$

For the real machine, one would, of course, have to take into account the I, BnL data of each individual quadrupole. The currents derived from the model and the real currents archived in typical SCR files (SR1998-062-0302-105314 used during the start-up period or SR 1997-238-0826-052204 used last September) are compared in Table 2.

Table 2

	$L_{mag\_th}$ (m)	$KnL_{mag\_th}$ ( $m^{-1}$ )	$I_{calib}$ (A)	$I_{SCR}$ (A)
Q1	0.5	-0.245589	226.579	226.441
Q2	0.8	0.558622	323.38	326.067
Q3	0.5	-0.281851	260.665	264.923
Q4	0.5	-0.404773	390.400	390.435
Q5	0.6	0.468082	368.824	369.037

The discrepancy between the model and the real currents concerns Q2 and Q3. It reflects the fact that these two families are used as "tune knobs" to adjust the tunes of the real machine to the desired 0.2/0.3 values. Applying the KnL corresponding to the real currents leads to a somewhat different optics with tunes at  $\nu_x = 35.64$ ,  $\nu_y = 19.68$ , and  $\beta_y$  functions that are significantly larger than the design ones ( $\beta_y = 1.8$  m in the centre of the straight section and  $\beta_y = 67$  m at the Q4 location).

Beta function measurements performed last September (Sept 8, Sept 15, and 22) also show the same trend, i.e., average  $\beta_y$  values larger than predicted. In addition, a significant modulation in the vertical plane is observed (Figure 5).

These differences tend to prove that the model presently used to describe the linear optics is not fully adequate to represent the machine. This might have an impact on real machine characteristics (mismatch of the achromat spoiling the horizontal emittance, dispersion distortions, beam size modification due to incorrect  $\beta$ -functions, etc.).

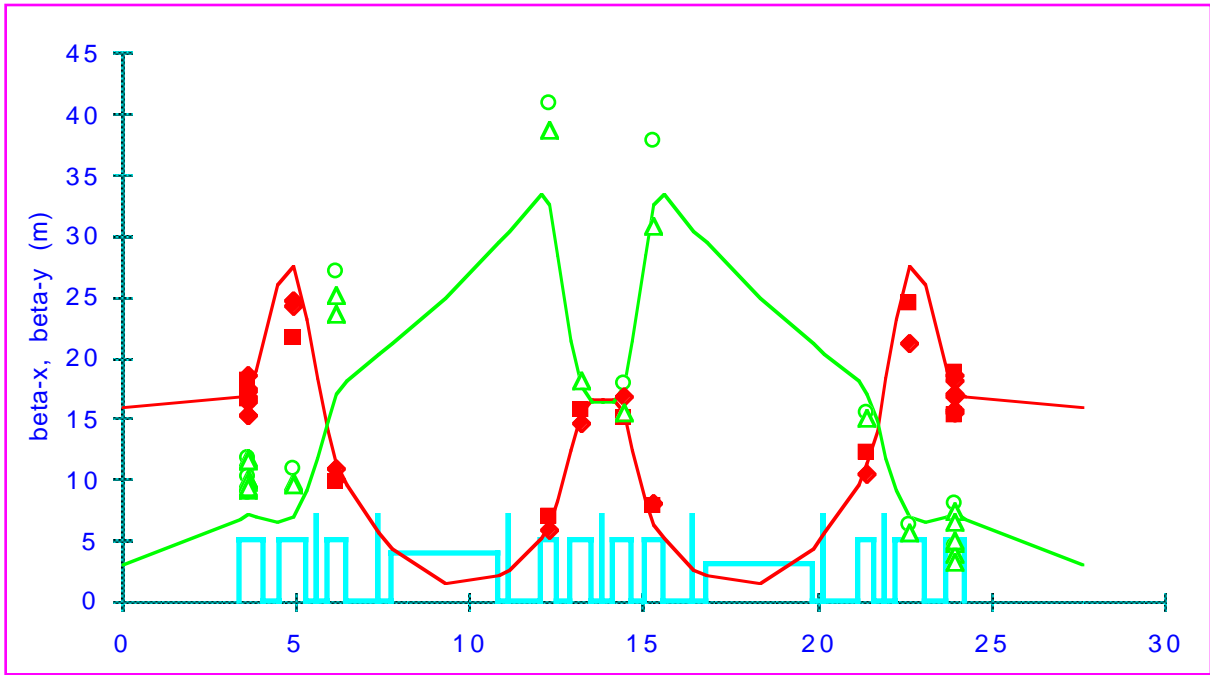


**Figure 5.** Comparison of the model and measured  $\beta$ -functions (Sept 1997)

### **Possible sources of incorrect modeling**

Several factors may account for an incorrect modeling:

#### *1. Uncertainties on magnetic lengths*

Given the strong focusing of the lattice, the optics description of replacing theoretical magnetic lengths ( $L_{\text{mag\_th}}$ ) with values updated from magnetic measurements ( $L_{\text{mag}}$ ) and readjusting the quadrupole strengths so that  $K \cdot L_{\text{mag\_th}} = K_{\text{mag}} \cdot L_{\text{mag}}$  is not precise enough. The change in lattice characteristics (optical functions are given in the centre of the straight section) is shown in Table 3. In order to restore lattice characteristics, a new model has been optimized (referred to as  $K_{\text{opt}}$  in Table 3).

Table 3

	$L_{mag\_th}$ (m)	$K$ (m <sup>-2</sup> )	$L_{mag}$ (m)	$K_{mag}$ (m <sup>-2</sup> )	$K_{opt}$ (m <sup>-2</sup> )
Q1	0.5	-0.491177	0.4935	-0.497646	-0.497411
Q2	0.8	0.698277	0.7924	0.704974	0.703711
Q3	0.5	-0.563701	0.4935	-0.571126	-0.569088
Q4	0.5	-0.809546	0.4900	-0.826067	-0.824691
Q5	0.6	0.780136	0.5915	0.791347	0.790130

	$K, L_{mag\_th}$	$K_{mag}, L_{mag}$	$K_{opt}, L_{mag}$
$v_x$	35.2	35.32	35.2
$v_y$	19.3	19.44	19.3
$\beta_x$ (m)	16.0	16.3	16.0
$\beta_z$ (m)	3.0	2.47	3.0
$\eta_x$ (mm)	0	-7.4	0

Except for Q1, the new model corresponds to rather significant different currents (Table 4).

Table 4

	model #1 $K, L_{mag\_th}$	model #2 $K_{mag} = \frac{KL_{mag\_th}}{L_{mag}}, L_{mag}$	model #3 $K_{opt}, L_{mag}$	$I_{SCR}$ (A)
Q1	226.58	226.58	226.47	226.44
Q2	323.38	323.38	322.76	326.07
Q3	260.67	260.67	259.71	264.92
Q4	390.40	390.40	389.48	390.44
Q5	368.82	368.82	368.11	369.04

Are the proposed magnetic lengths really correct? In order to minimize the resulting imprecisions in the model, the following method could be used:

- make 2-D computations of the central gradient  $G_0$  as a function of current for the different types of quadrupoles and get computed tables  $G_0(n), I(n)$
- interpolate  $G$  for the actual current  $I$  as:  $G = G_0(n) + \frac{G_0(n+1) - G_0(n)}{I(n+1) - I(n)} [I - I(n)]$
- derive the magnetic length as:  $L_{mag} = \frac{BnL}{G}$

## 2. *Random gradient errors in quadrupoles*

The pollution introduced by gradient errors leads to a modification of the tunes and a modulation of the  $\beta$ -functions. Powering the quadrupoles individually is supposed to compensate for these gradient errors. Therefore, unless something is going wrong with the magnetic measurements or the calibration of the power supplies, both modulation and tune changes should be negligible.

It can, however, be anticipated that some residual errors are still present. The effect of these errors is described in Table 5 and Figure 6, assuming that they are randomly distributed with Gaussian distributions ( $\sigma_{\Delta G/G}$ ). Due to the increased vertical focusing of the low  $\beta_y$  optics, the sensitivity to these errors is larger in the vertical plane than for the  $\nu_y = 14.3$ ,  $N = 40$  optics. The modulation starts to be significant for large residual errors ( $\sigma_{\Delta G/G} = 1.0 \cdot 10^{-3}$ , i.e., a value of the same order as the raw gradient errors). Also the behaviour does not fit experimental observations since the modulation is larger in the horizontal plane than in the vertical one.

Table 5

$\sigma_{\Delta G/G}$	average $\nu_x$	$\sigma_{\nu_x}$	average $\nu_y$	$\sigma_{\nu_y}$
$2.5 \cdot 10^{-4}$	0.1990	$2.8 \cdot 10^{-3}$	0.2995	$2.0 \cdot 10^{-3}$
$5.0 \cdot 10^{-4}$	0.1985	$6.9 \cdot 10^{-3}$	0.2970	$4.9 \cdot 10^{-3}$
$7.5 \cdot 10^{-4}$	0.1980	$1.0 \cdot 10^{-2}$	0.2949	$7.4 \cdot 10^{-3}$
$1.0 \cdot 10^{-3}$	0.1976	$1.4 \cdot 10^{-2}$	0.2928	$1.0 \cdot 10^{-3}$

## 3. *Gradient errors in a single quadrupole*

Such an error could come from either the magnet itself or from a wrong calibration or operating conditions of the associated power supply. The sensitivity of the machine to such errors is sketched in Table 6 with the  $\beta$ -beat defined as:  $\max(\frac{\beta_{min} - \beta_{model}}{\beta_{model}}, \frac{\beta_{max} - \beta_{model}}{\beta_{model}})$ , with the  $\beta$ s taken in the middle of the straight sections. A Q4 quadrupole could be a possible candidate: a gradient error produces almost no modulation in the horizontal plane but a significant one in the vertical plane, as experimentally observed (Figure 7). In addition, the resulting dispersion pattern is very similar to the measured one (see Figure 8). However, it has to be recalled that other kinds of errors could produce identical patterns which reflect the beat between the ring periodicity (40) and the horizontal betatron frequency (35).

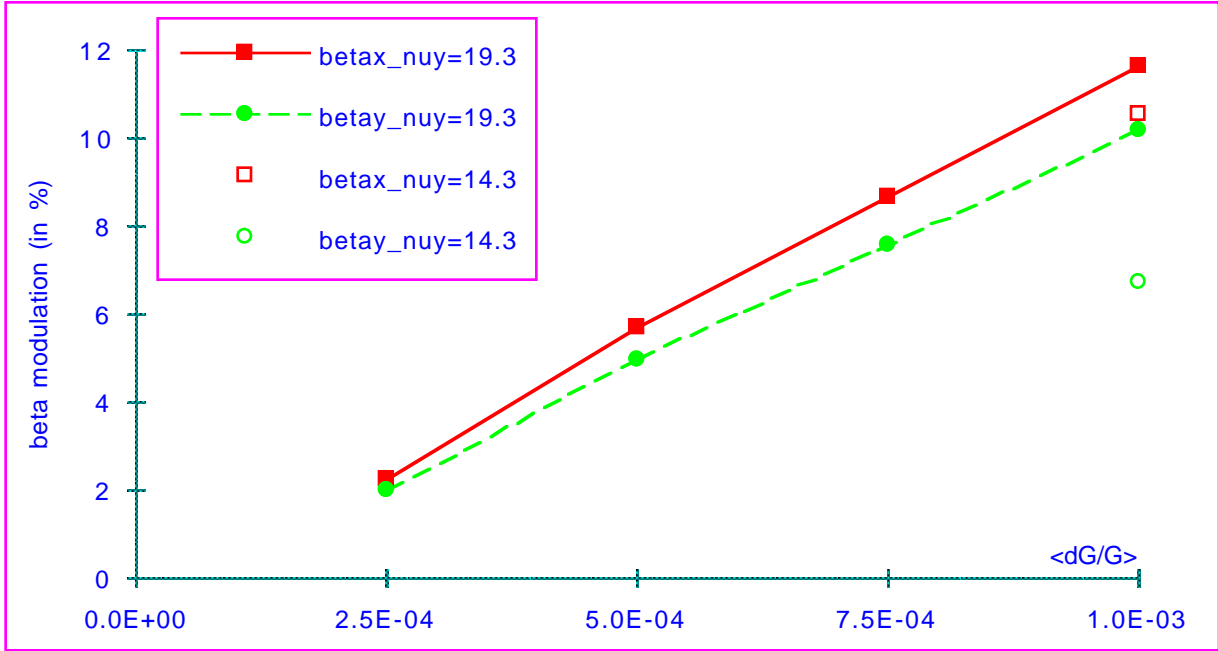


Figure 6.  $\beta$ -function modulation with residual gradient errors

Table 6

	$\Delta G/G$ (%)	$\beta_x$ beat (%)	$\beta_y$ beat (%)	$\Delta v_x$	$\Delta v_y$
Q1	10	28.2	9.8	-0.035	0.014
Q2	2	16	22.4	0.023	-0.006
Q3	10	20	31.8	-0.027	0.04
Q4	4	5.8	36.0	-0.008	0.044
Q5	4	15.4	18.6	0.022	-0.026

Unfortunately, this scenario does not explain the 14-A change in the Q1 family current required at the beginning of the run since the tune readjustment to nominal values would only imply a change in the Q1 family by about  $8 \cdot 10^{-4}$  together with a fine retuning of Q2 and Q3.

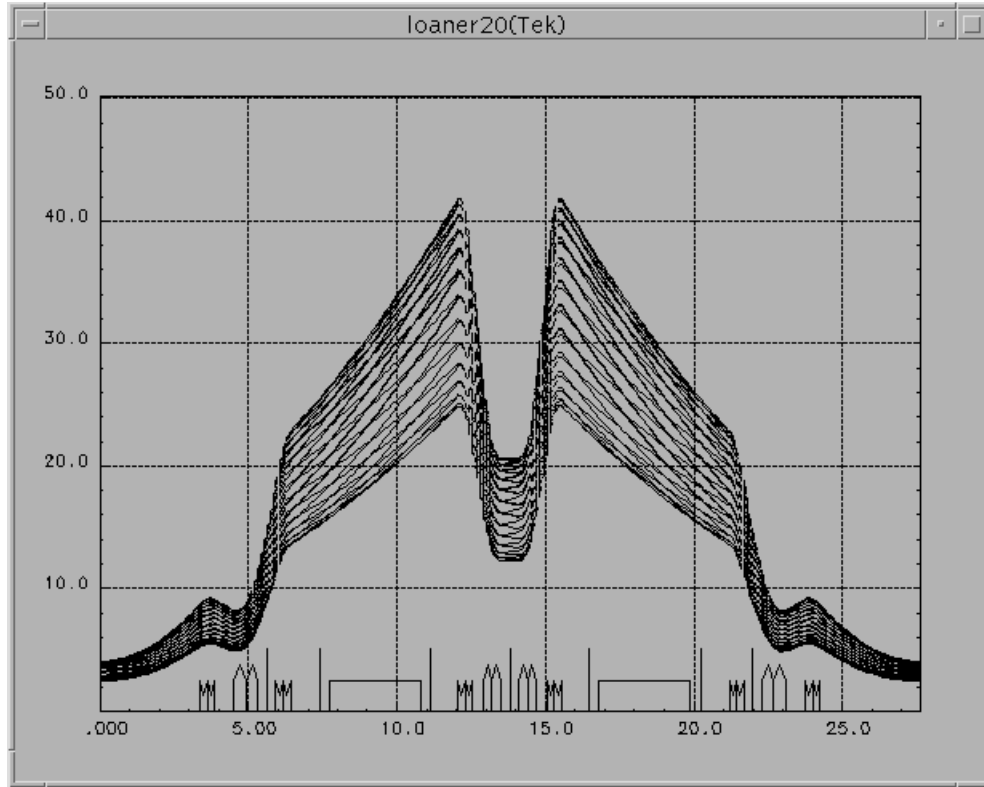
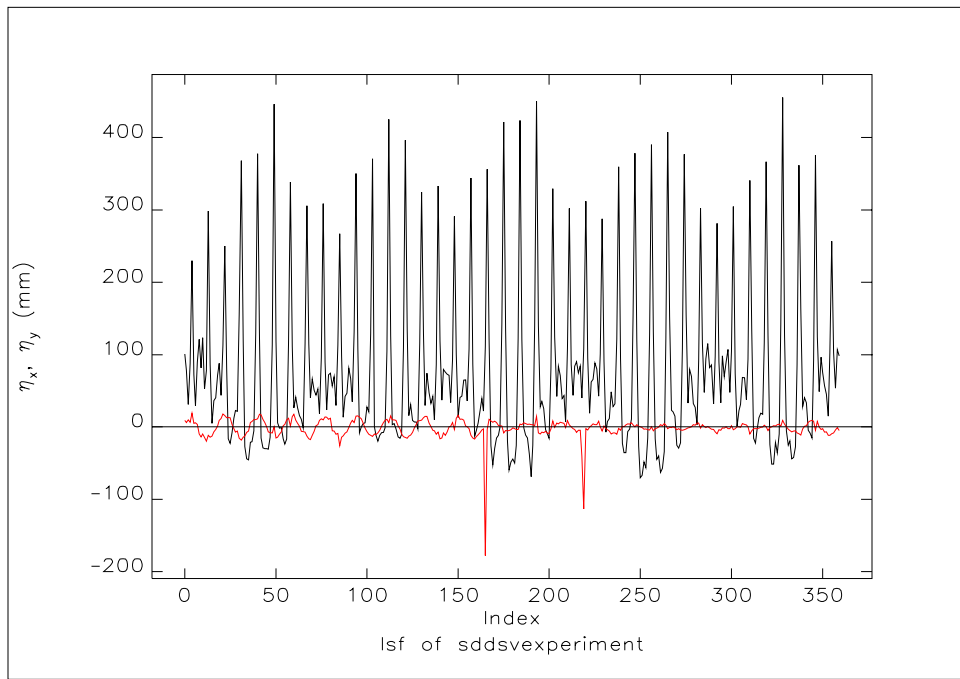
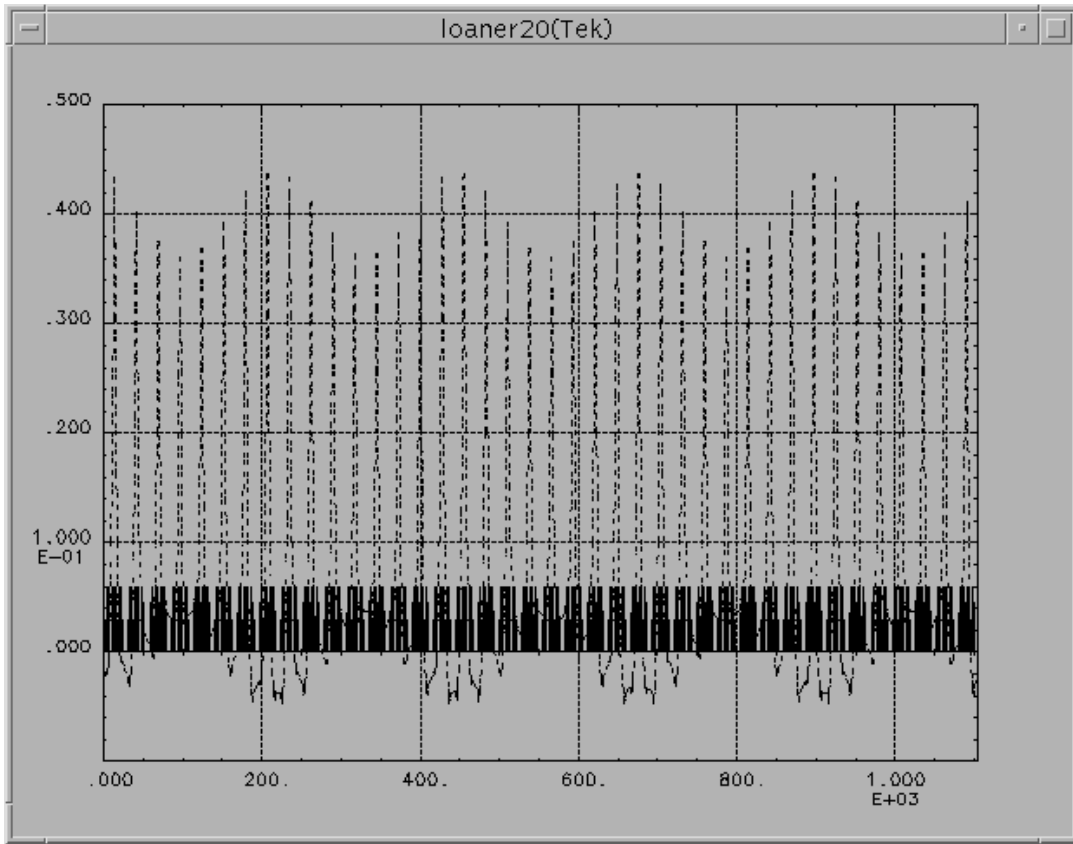


Figure 7. Vertical  $\beta$  modulation induced by a single Q4 gradient error

#### 4. Validity of $\beta$ -function measurements

Since the  $\beta$ -function measurement procedure is based on the tune change induced by increasing the current of a single quadrupole by 10 A in several steps, one may question how the modulation introduced by this intentional gradient error can affect the interpretation of the measurement. Predictions from simulations are summarized in Table 7 for each quadrupole and compared to some of the experimental results (S35A:Qn quadrupoles measured on Sept 15). The modulation in the horizontal/vertical plane is computed as the relative difference between the modified  $\beta$ -function in the centre of the quadrupole and the design one.



**Figure 8.** Dispersion pattern generated by a Q4 gradient error compared to the dispersion pattern from measurements

Table 7

	$\Delta G/G$ (%)	mod x (%)	mod y (%)	$\Delta \nu_x$ theor	$\Delta \nu_y$ theor	$\Delta \nu_x$ meas	$\Delta \nu_y$ meas
Q1	4.34	3.8	1.3	-0.015	0.006	-0.014	0.009
Q2	2.84	-4.7	-1.4	0.032	-0.009	0.031	-0.013
Q3	3.66	2.3	3.3	-0.01	0.014	-0.008	0.021
Q4	1.78	0.9	4.8	-0.004	0.019	-0.005	0.022
Q5	2.12	-2.3	-2.4	0.012	-0.014	0.013	-0.015

Of course, modifications of the  $\beta$ -functions by a few % occur during the measurements. But since the measured changes in tunes are very close to expectations, the determination of the unperturbed  $\beta$ -function should not be spoiled. However, given the fact that some of the tune shifts ( $\Delta \nu_y$  for Q1 and Q2,  $\Delta \nu_x$  for Q3 and Q4) are very small, any tune motion due to some noise source could significantly affect the results of the corresponding  $\beta$  values, the relative error on  $\beta$  being equal to the relative error on  $\Delta \nu$ .

Ideally, the  $\Delta I$  applied to each quadrupole for each plane should be individualized and large enough to make the tune jitter contribution negligible. In the case of increasing  $\Delta \nu$ , the approximate formula  $\Delta \nu = \frac{1}{4\pi} \beta_0 \Delta KL$  has to be replaced by the exact one relating the unperturbed machine ( $\beta_0, \nu_0$ ) to the perturbed one ( $\nu$ ):  $\beta_0 = \frac{2 \cos(2\pi \nu_0) - 2 \cos(2\pi \nu)}{\Delta KL \sin(2\pi \nu_0)}$ . With the present  $\Delta \nu$ , the introduced imprecision is less than 1 m in the worse case ( $\beta_y$  for Q4) but could start to be significant with larger  $\Delta I$ .

Can we neglect the non-reproducibility of quadrupole strengths due to hysteresis when changing the current? The procedure that is used aims at restoring the tunes after a measurement. It is expected that this method minimizes the detrimental effects. Even if residual gradient errors remain, their amplitude and therefore the resulting perturbation should be a small fraction of the effects quoted in Table 6.

##### 5. *Positioning errors of quadrupoles*

Longitudinal misalignments of quadrupoles also generate additional focusing effects. But as shown in Figure 9, the modulation produced by different sets of positioning errors with an rms of  $\sigma_s = 5$  mm is more or less equivalent in both planes and does not fit the experimental observations.

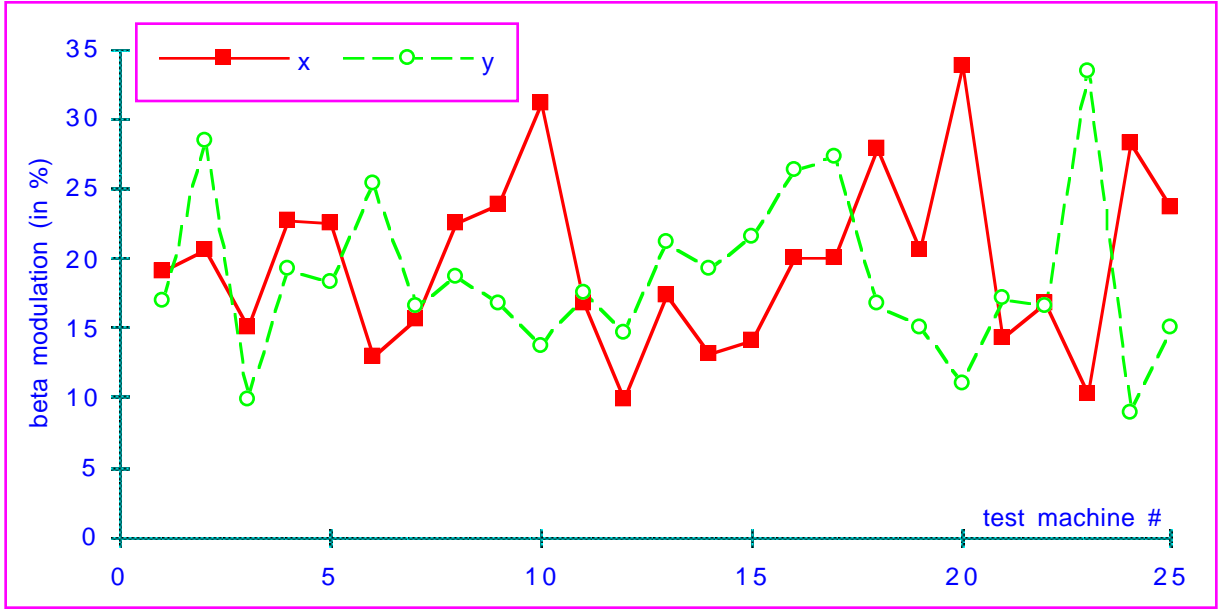


Figure 9.  $\beta$ -modulation produced by random longitudinal quadrupole misalignments

#### 6. Closed orbit errors in sextupoles

These errors are also responsible for additional focusing. Some comparisons have been made as a function of the residual closed orbit distortions in the machine (expressed as the rms value at the BPM locations) and of the strength of sextupoles. The procedure consists of generating closed orbit errors with quadrupole misalignments (typically  $\sigma_x = \sigma_y = 40 \mu\text{m}$ ) and applying a SVD correction using the H2 (for x-plane) and the A:V2 and B:V3 (for y-plane) correctors with a variable number of eigenvectors (6/4 for rms orbits in the 0.5/0.4-mm range, 60/40 for rms orbits in the 0.1-mm range). The results of these simulations are summarized in Table 8 and Figures 10 and 11.

Table 8

$\sigma_x / \sigma_y$ (mm)	average $\nu_x$	$\sigma_{\nu_x}$	average $\nu_y$	$\sigma_{\nu_y}$
0.1 / 0.12 standard sextupoles	0.2044	$5.45 \cdot 10^{-3}$	0.3098	$1.2 \cdot 10^{-2}$
0.5 / 0.4 standard sextupoles	0.1985	$6.9 \cdot 10^{-3}$	0.2970	$4.9 \cdot 10^{-3}$
0.5 / 0.4 S1 = S2 = 0	0.2178	$3.4 \cdot 10^{-2}$	0.3087	$2.1 \cdot 10^{-2}$
0.5 / 0.4 S1 = S2 = 0, $\xi_{x,y} = 0$	0.2172	$3.2 \cdot 10^{-2}$	0.3073	$1.8 \cdot 10^{-2}$

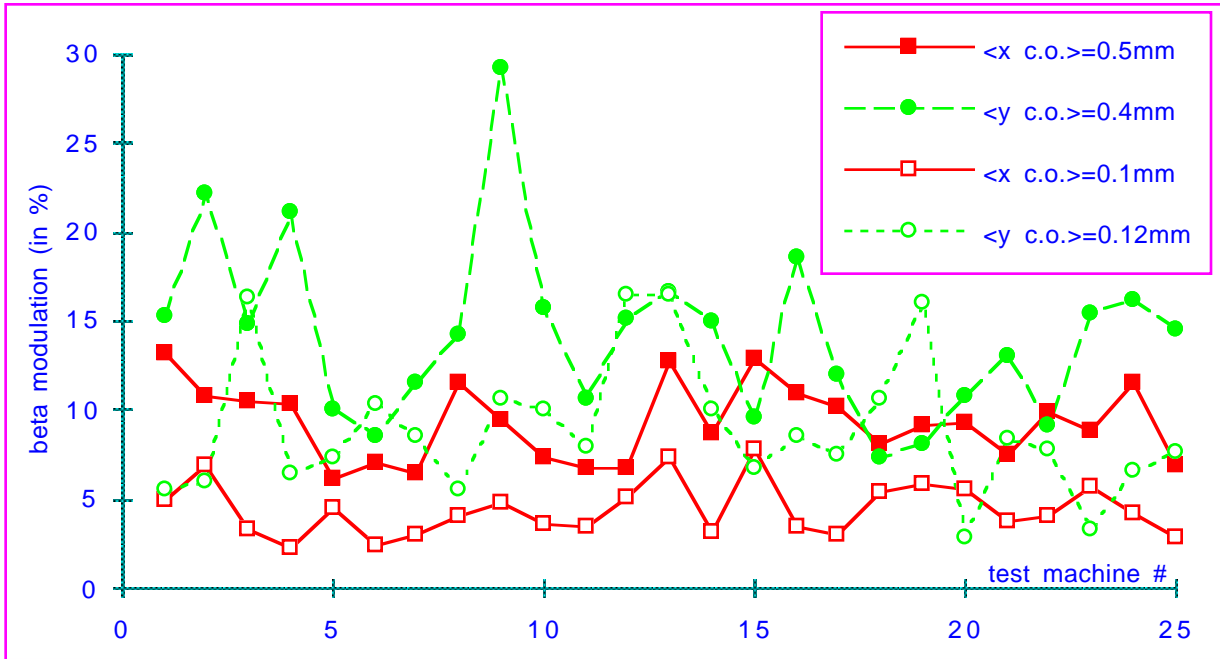


Figure 10. Evolution of the  $\beta$ -function modulation with residual closed orbits

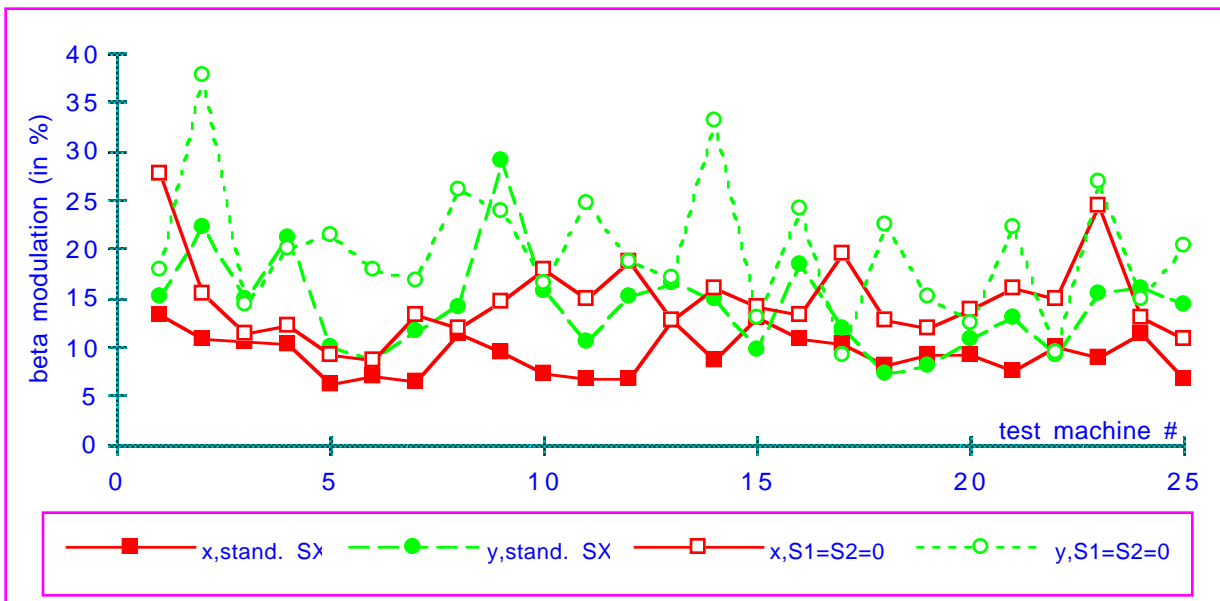


Figure 11. Evolution of the  $\beta$ -function modulation with sextupole settings

It must be pointed out that the closed orbit patterns used in simulations are not identical to the user orbit since no steering is performed in the straight sections. However, the orbit offsets at the sextupole locations look qualitatively equivalent and therefore should induce the same distortions. Clearly, large orbits produce significant modulations of  $\beta$ -functions. Even if the

modulation is larger in the vertical plane, the contrast between the horizontal and the vertical modulation is not as large as experimentally observed. Ideally, however, modeling-related  $\beta$ -function measurements should be done with steering the beam to zero setpoints.

The harmful effects of the off-centered orbits in sextupoles are mainly due to the chromaticity correcting sextupoles:

- switching off the harmonic sextupoles does not reduce the modulation by much. This is due to the fact that the compensating effects of these sextupoles are no longer present.
- decreasing the chromaticity to zero (which could be very difficult on the real machine) changes the sextupole strengths very little as compared to the strengths required for chromaticity compensation. Therefore, the modulation is hardly reduced.

## **Modeling of the linear optics from the $\beta$ -functions measurements**

### *1. Method*

At the start-up of the run,  $\beta$ -functions (mainly at the Q1 and Q4 locations) were measured with varying Q1 in order to minimize the observed distortions in the vertical plane. Measurements performed in September 1997 are also available.

For each set of data, the strengths of the Q1, Q2, and Q3 quadrupoles of the model were fitted in order to minimize the differences between the model (ideal 40-fold symmetry lattice) and the average measured  $\beta$ -functions and to reproduce the experimental tunes. It is assumed that the lattice has the mirror symmetry about the centre of the achromat so that average  $\beta$ -functions are determined from the measurements at the A:Qn and B:Qn quadrupoles. This averaging is correct to first order, provided the number of measurements is large enough to sample several periods of oscillations of the  $\beta$ -function (this is not the case for most of the measurements and therefore the average value can be under- or overestimated). The larger the modulation, the larger the error on the average  $\beta$ . The model was either the one with predicted magnetic lengths or the one with updated magnetic lengths. This gives a series of three parameters to fit, most of the time, six data points (2 tunes + 2 horizontal and 2 vertical  $\beta$ s at the Q1 and Q4).

### *2. Analysis*

The  $\beta$ -functions corresponding to the new model (dotted lines) are compared to those of the initial model (plain lines) and to the measured values, and are plotted for two extreme cases: Mar 2 measurements with nominal Q1 (Figure 12) and Mar 4 measurements with +14 A on Q1 (Figure 13).

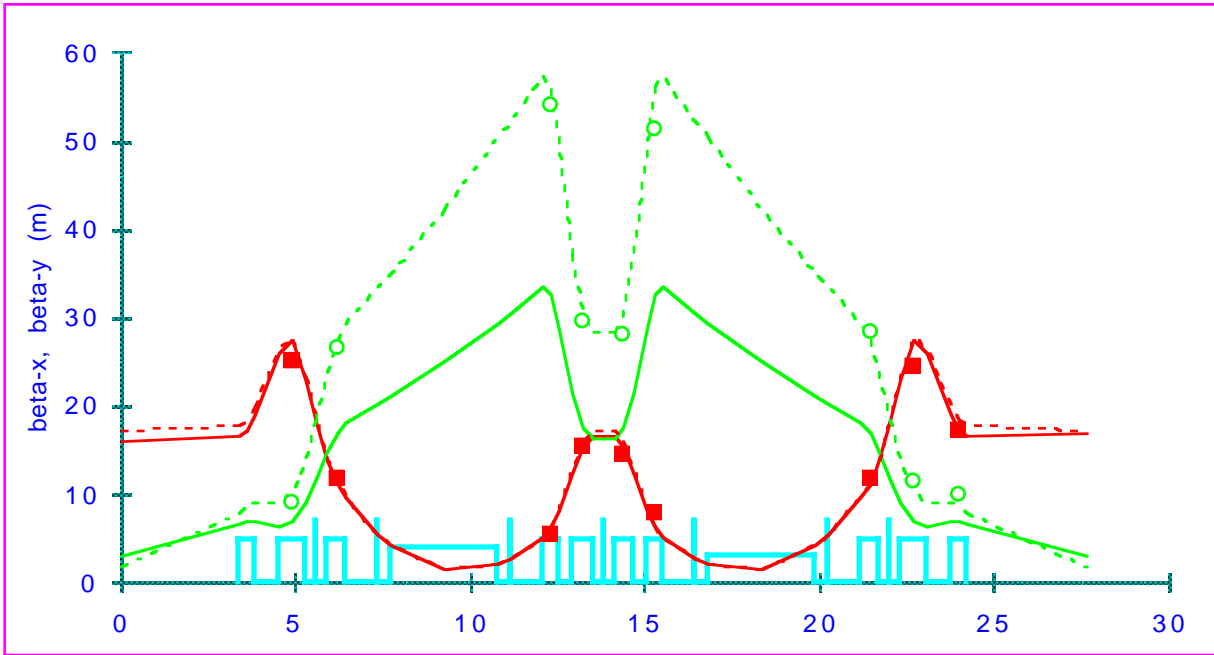


Figure 12. Modeling of the Mar 2  $\beta$ -function measurements

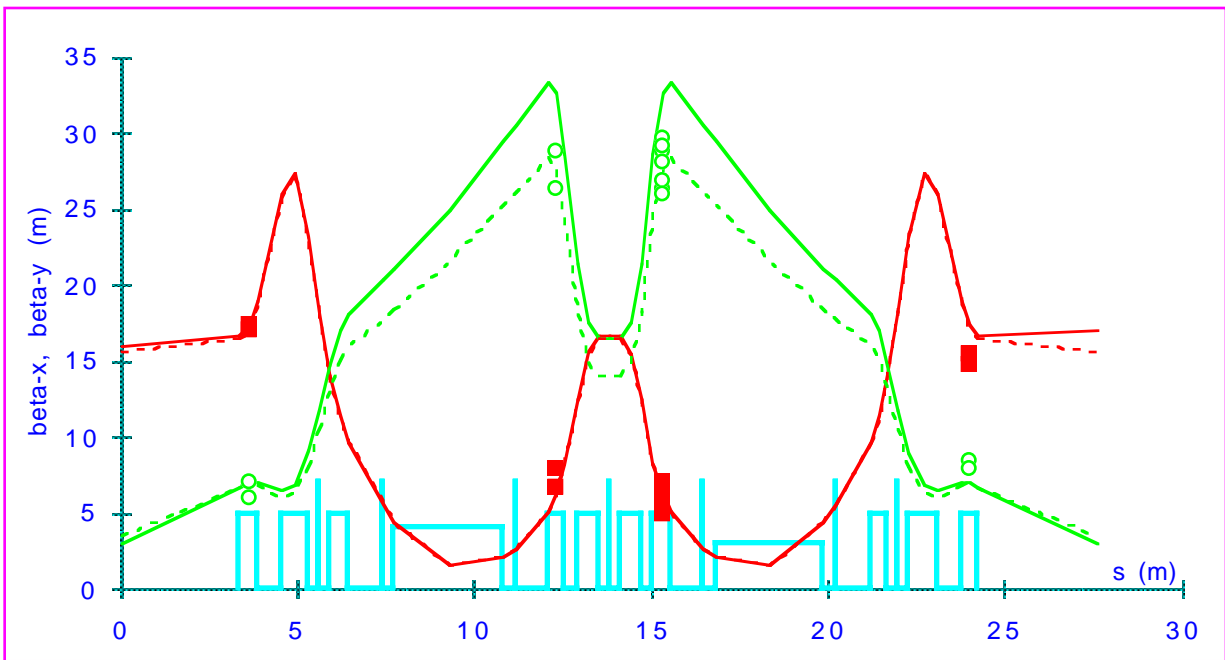


Figure 13. Modeling of the Mar 4  $\beta$ -function measurements

The convergence of the fit can be compared in the different cases via the value of the  $\chi^2$  function that quantifies the deviations between the actual optics and the measurements. This quantity is expressed as

$$\chi^2 = \sum_1^{N_{meas}} \left( \frac{\beta_{mod\ el} - \beta_{meas}}{0.01 * \beta_{mod\ el}} \right)^2 + \sum_1^2 \left( \frac{v_{mod\ el} - v_{meas}}{0.0001 * v_{mod\ el}} \right)^2.$$

The quality of the fit is summarized in Table 9. Models were fitted for both the design and the updated magnetic lengths with Q1, Q2, Q3 as fitting parameters. Attempts were also made after adding Q4 and Q5 as parameters. Although the fits look globally better with these additional parameters, they lead to a mismatch of the achromat and a significant positive dispersion in the straight sections and therefore do not look very realistic. Adding a zero-dispersion constraint in the straight sections should give more credible fits. It must also be noted that fits give equivalent convergence for the design and updated magnetic lengths. The larger  $\chi^2$  for the models with nominal Q1 are due to the larger number of constraints.

Table 9

	design magnetic lengths		updated magnetic lengths	
	Q1-Q2-Q3	Q1 --> Q5	Q1-Q2-Q3	Q1 --> Q5
nominal Q1_Mar2 *	3.9 10 <sup>3</sup>	2.7 10 <sup>3</sup>	4.6 10 <sup>2</sup>	4.1 10 <sup>2</sup>
$\Delta I_{Q1} = -5$ A	1.5 10 <sup>2</sup>	6.4 10 <sup>1</sup>	1.5 10 <sup>2</sup>	6.5 10 <sup>1</sup>
$\Delta I_{Q1} = +6$ A	8.9 10 <sup>1</sup>	6.4 10 <sup>1</sup>	8.2 10 <sup>1</sup>	5.9 10 <sup>1</sup>
$\Delta I_{Q1} = +10$ A	1.1 10 <sup>2</sup>	1.0 10 <sup>2</sup>	1.1 10 <sup>2</sup>	1.0 10 <sup>2</sup>
$\Delta I_{Q1} = +14$ A	6.6 10 <sup>1</sup>	3.4 10 <sup>1</sup>	6.3 10 <sup>1</sup>	3.3 10 <sup>1</sup>
nominal Q1_Sep8 *	1.5 10 <sup>3</sup>	8.9 10 <sup>2</sup>	1.4 10 <sup>3</sup>	8.8 10 <sup>2</sup>
nominal Q1_Sep15&22 *	8.7 10 <sup>2</sup>	2.9 10 <sup>2</sup>	8.8 10 <sup>2</sup>	2.9 10 <sup>2</sup>

\* additional  $\beta$ -function measurements at Q2, Q3, Q5

### 3. Calibration of quadrupoles

As mentioned earlier, for each new optics resulting from the fit of measured  $\beta$ -functions, a set of quadrupole currents can be derived from the KnL values. The credibility of this procedure relies on the absolute calibration of the measuring coil and on the knowledge of the machine energy. In order to take into account possible uncertainties in those two quantities, a fudge factor (referred as *coef*) is introduced in the following way:

$$BnL = \frac{K_{opt} L_{mag} * B\rho}{coef}$$

$$I = I_{meas}(n) + \frac{I_{meas}(n+1) - I_{meas}(n)}{BnL_{meas}(n+1) - BnL_{meas}(n)} [BnL - BnL_{meas}(n)]$$

Ideally the fudge factors should be identical and equal to 1 for all families. In practice, different sets have to be defined for each model to enable the interpolated quadrupole currents to match the experimental ones. Figure 14 shows the results of the modeling of the measurements.

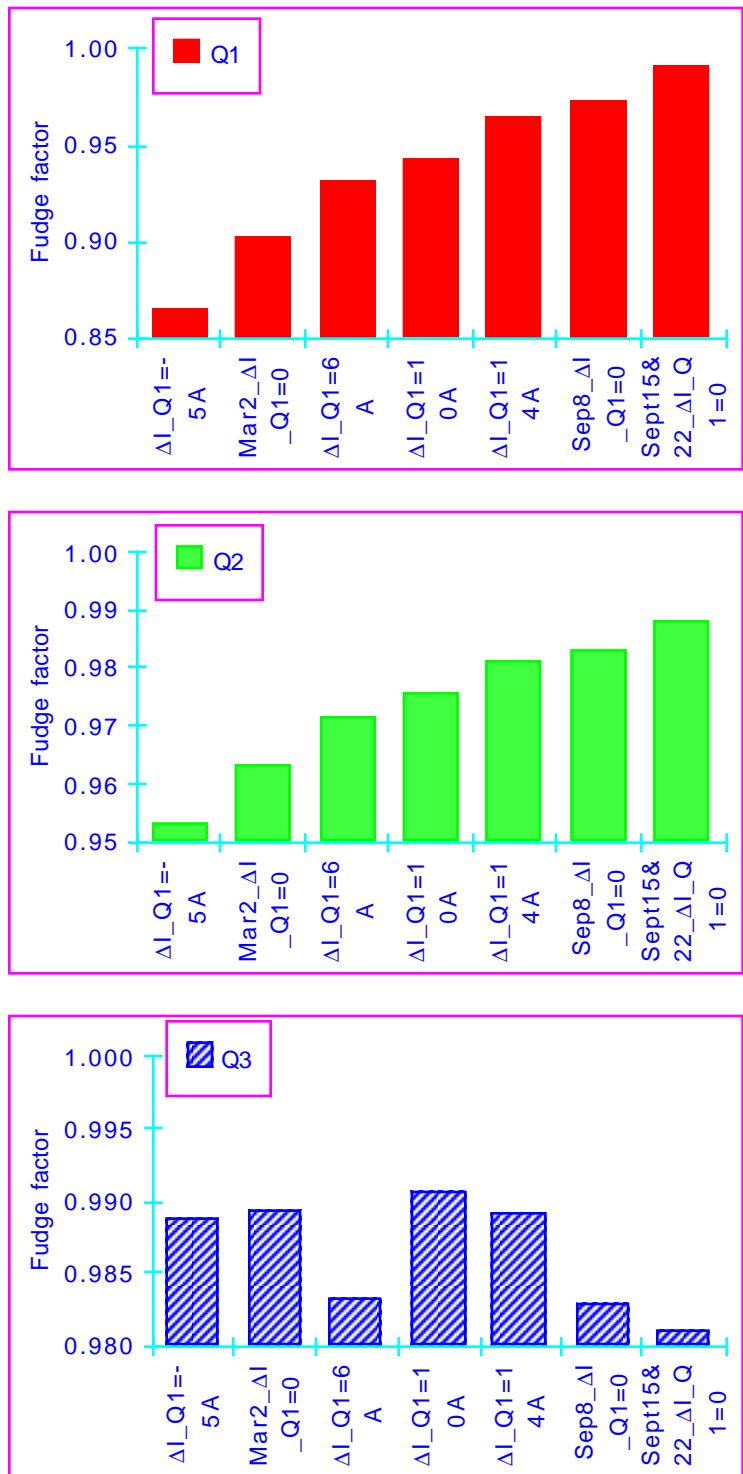


Figure 14. Fudge factors resulting from the modeling of measured  $\beta$ -functions

They are clearly inconsistent: fudge factors are very far from 1 and, surprisingly, vary linearly with  $\Delta Q_1$ . For comparison, the results of September 1997 appear more realistic (Figure 15).

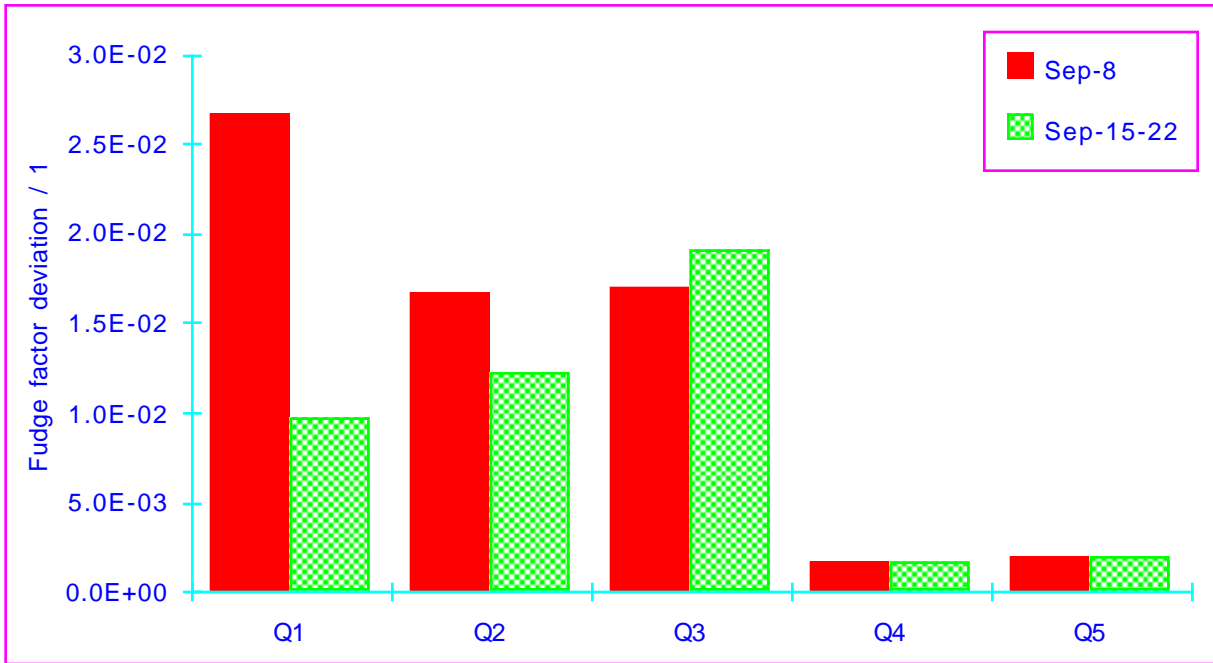


Figure 15. Fudge factors deduced from September 1997 measurements

### **Effects of the closed orbit on the modeling**

All the measurements analyzed so far were performed with the beam steered to the user orbit. In order to eliminate some of the imprecisions linked to the induced  $\beta$ -modulation, a series of measurements were performed when steering the beam to zero setpoints.

#### *1. Mar 23 data*

An attempt to steer the P2-P5 to zero setpoints in the horizontal plane using the H2 + the B:H4 correctors and punching down the unwanted correctors led to a change in all the setpoints from 0 to 0.75 mm in steps (to compensate for a clear offset of all BPMs) and an alteration of the rf frequency by about 350 Hz. An orbit of the order of 0.3 mm rms was obtained, but a later analysis indicates that the procedure had brought the beam off-axis by about 0.8 mm. The dependence of lattice characteristics upon momentum deviations makes a comparative analysis of these measurements with data taken with the user orbit more difficult. In the vertical plane, a 0.3-mm rms orbit was obtained with the A:V2 and B:V3 correctors.

Two series of measurements were done with this orbit:

- average  $\beta$ -function measurements. The procedure consists of changing the current in a family of quadrupoles (A, B or both) by  $\Delta I / N_{\text{magnets}}$  (with typically  $\Delta I = 10$  A) and deriving average  $\beta$ -functions from the induced tune shifts.
- individual  $\beta$ -function measurements in a full sector (35).

After having switched the steering back to the user orbit, the following measurements were done:

- average  $\beta$ -function measurements
- individual  $\beta$ -function measurements on A:Q4 and B:Q4 in sector 35

No standardization was done in the course of the measurements. The results of these measurements are plotted in Figure 16.

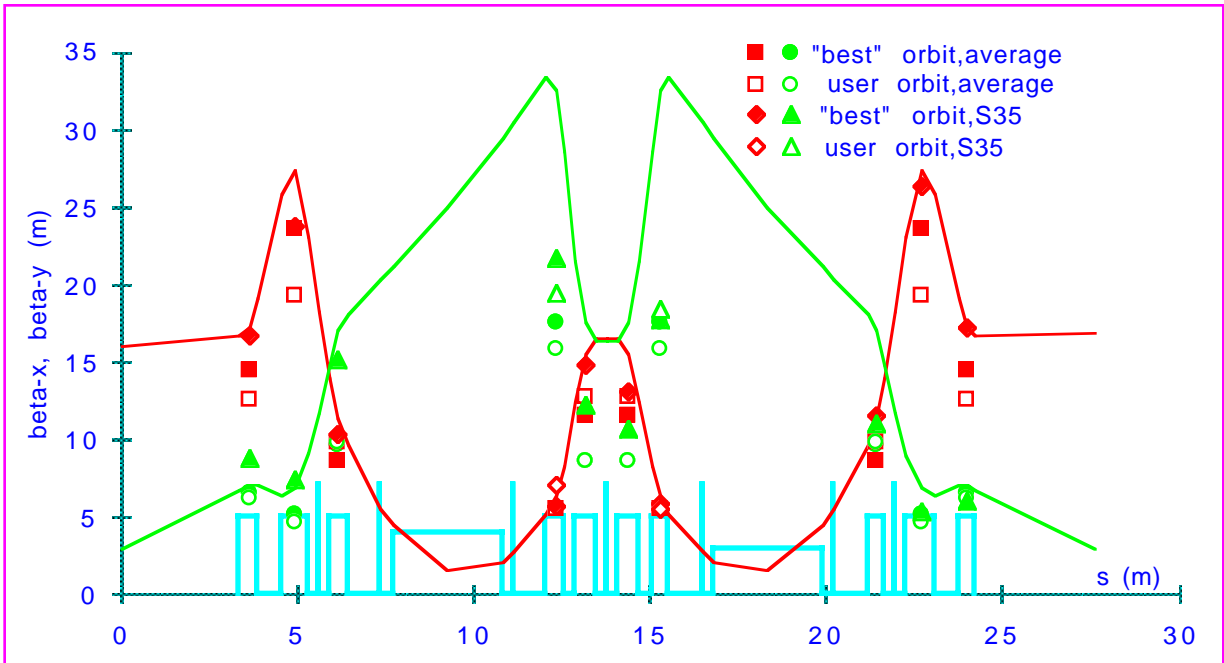


Figure 16. Average and individual  $\beta$ -function measurements with two different orbits

As already mentioned, it is difficult to compare the average  $\beta$ -functions for the two orbits because of the off-centering of the "best" orbit. However, there is a general and surprising tendency towards lower vertical  $\beta$ s as compared to the last measurements on Mar 4. This is also confirmed by the individual measurements. From the evolution of  $\beta_y$  at the Q4, which is summarized in Figure 17 (data at the A:Q4 and B:Q4 have been averaged), could we conclude that the unidentified cause that triggered the change of Q1 by 14 A has evolved and that it would be necessary to step back in Q1?

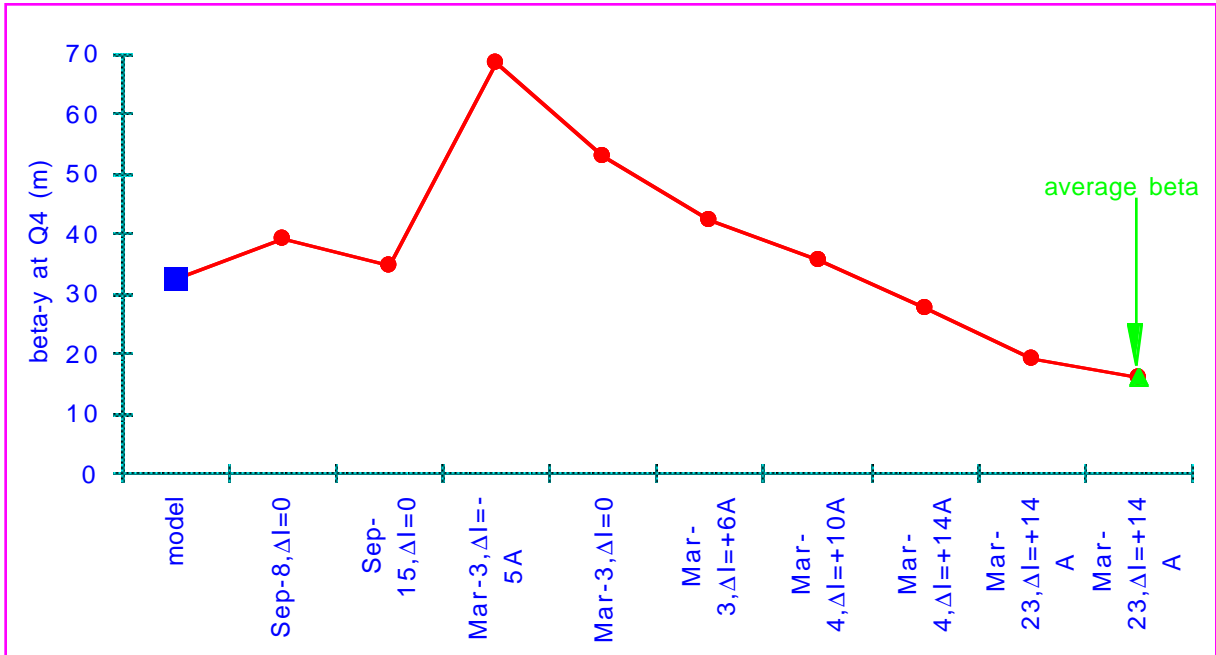


Figure 17. Evolution of  $\beta_y$  at the Q4

As far as local modulation is concerned, there are significant differences, even in the horizontal plane, between the average  $\beta$ -functions and the individual ones. More statistics on individual measurements are needed before drawing conclusions on the modulation and credibility of average  $\beta$ -function measurements. In particular, given the small increments in current for the individual quadrupoles (0.125 A), cumulative errors in the readbacks might have a strong impact on the precision of the measurement.

Attempts to define a model from the measured  $\beta$ -values give a very moderate fit (as shown in Figure 18), contrary to what is obtained from the individual  $\beta$ -function measurements. This would tend to prove that the data are not fully consistent.

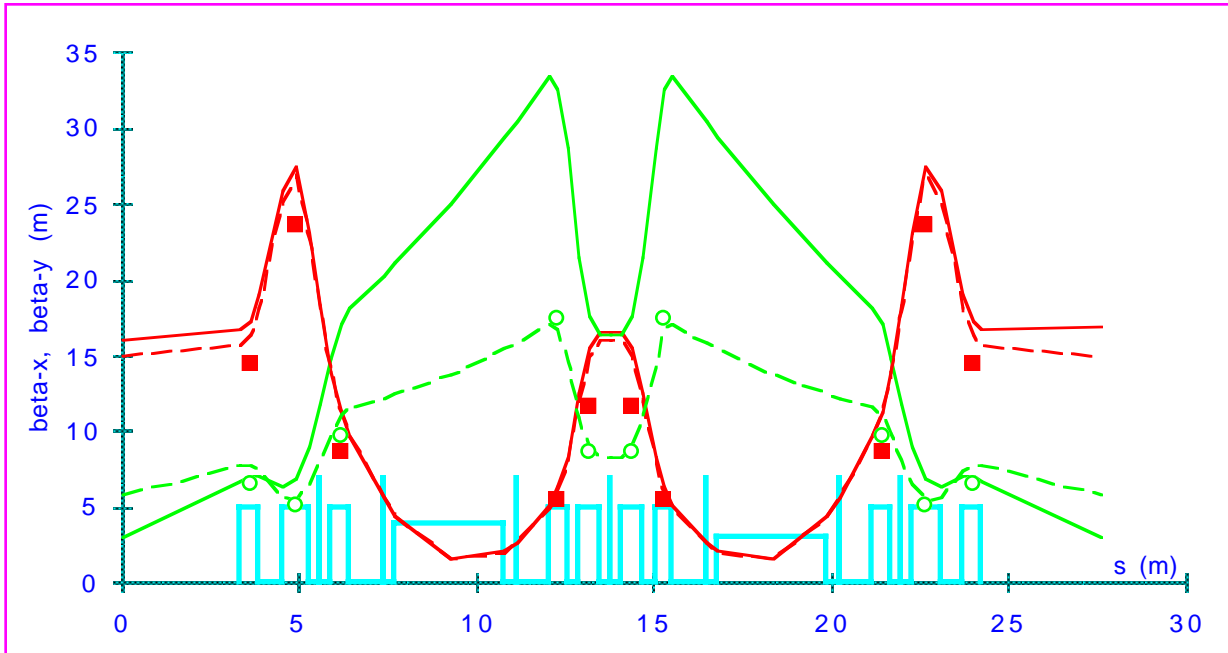


Figure 18. Modeling of the average- $\beta$  function measurements

## 2. Mar 30 data

The closed-orbit correction procedure was reviewed so that the horizontal orbit remained on axis with an rms of the order of 0.3 mm. However the sampling of the S4 sextupole offsets performed earlier in the day indicated that the orbit could reach up to 2 mm in some sextupoles. The standard set of correctors was used (no corrector in the dispersive sections) and unwanted correctors punched down, thus allowing the maximum strength to be reduced by more than a factor of 3 in the horizontal plane and a factor of 2 in the vertical plane. The remaining orbit at the P5 had an average of about -0.1 mm. This was left unchanged since the correction by the rf would have further increased the 0.15 mm average seen on all BPMs. In the vertical plane, the orbit was about 0.27 mm rms.

In these conditions (100 mA in 6 bunches + 25 triplets, initial tunes at  $\nu_x = 35.1956$ ,  $\nu_y = 19.2774$ ), several sets of  $\beta$ -functions were measured:

- A:Q4  $\beta$  measurements for all odd-numbered sectors
- A:Q3 and A:Q1  $\beta$  measurements for every 4<sup>th</sup> odd-numbered sector (1, 5, 9,...)
- average  $\beta$  measurements for all quadrupole families (A and B)

Late in the measuring sequence it was realized that the sextupole S20A:S4 had been left at 0 A, following the sextupole offsets measurements (in fact, the dramatic reduction in lifetime shown

in Figure 19 should have been a much earlier warning). In order to compare the measured values in similar conditions, the sextupole was left at 0 till the end of the centered orbit measurements. Since the orbit in the sextupole had been formally measured at about -0.09 mm, it can be assumed that the extra focusing from the off-centered orbit is negligible.

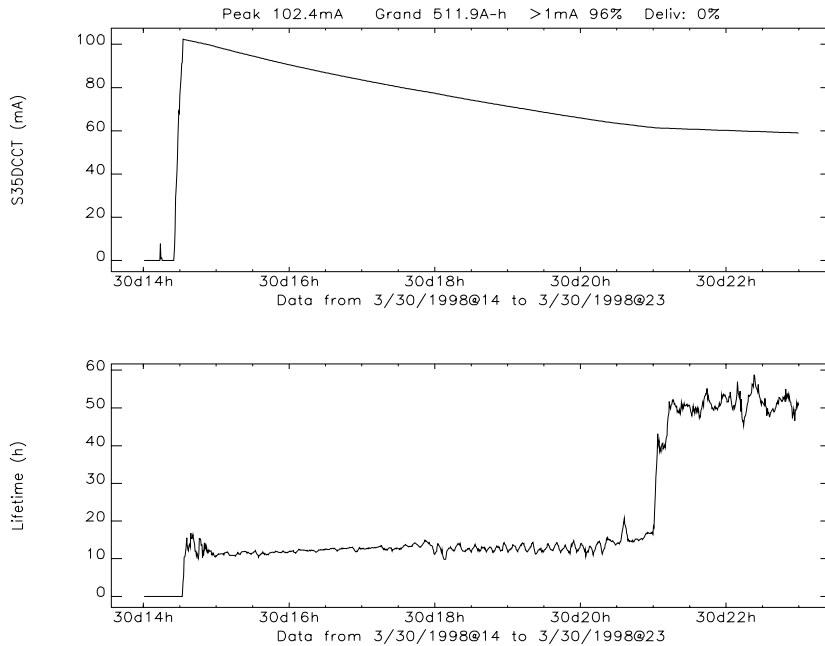
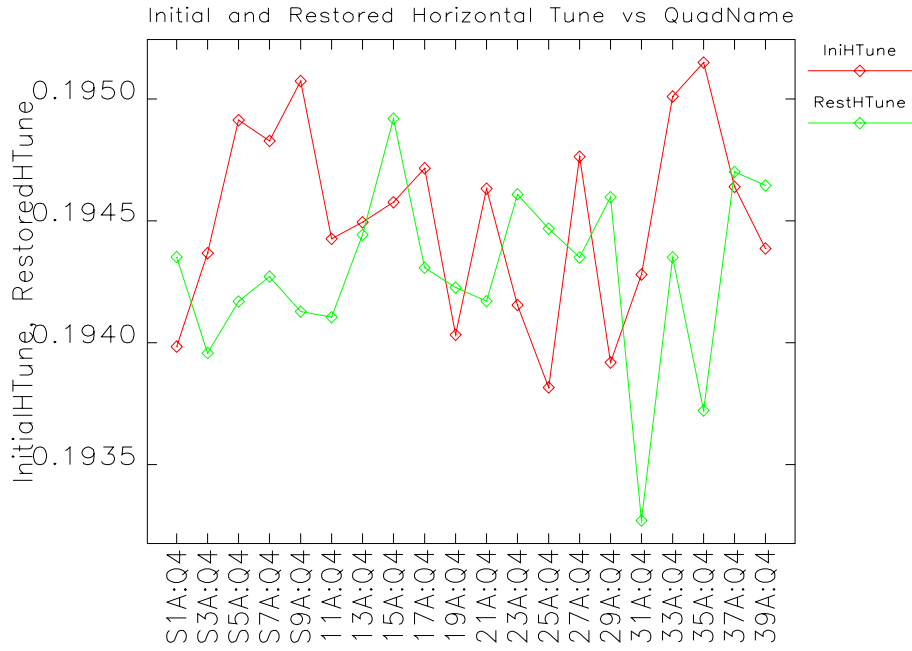
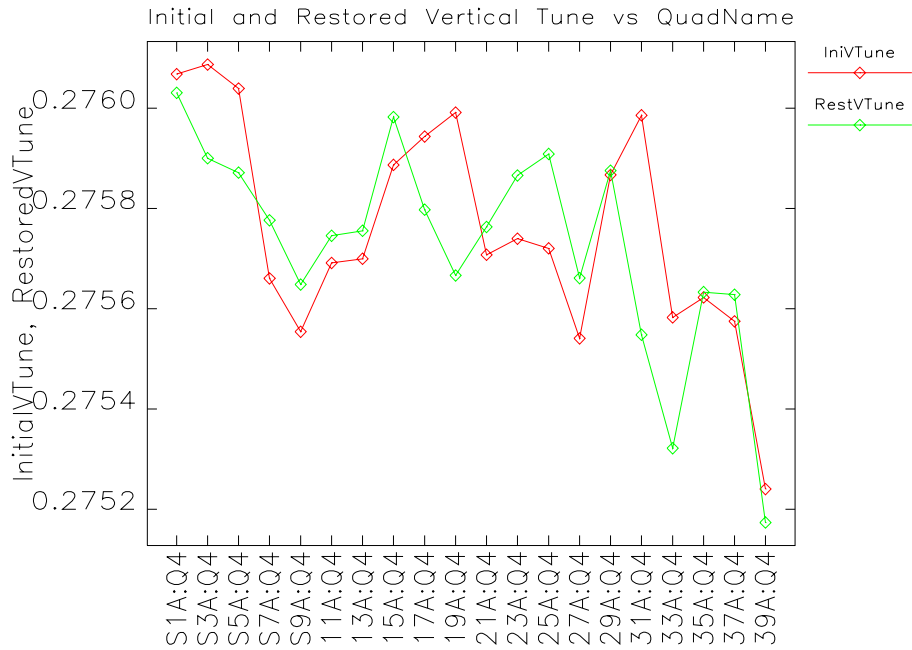


Figure 19. Lifetime evolution during the measurements with the effect of restoring S20:A S4

Magnets were not restandardized in the course of the measurements. However, as shown in Figure 20 and 21 for the A:Q1 series, the restoration of tunes after each measurement via the application of a reverse bias current is very good and there should be no induced distortions of the optics.



**Figure 20.** Initial and restored horizontal tunes



**Figure 21.** Initial and restored vertical tunes

Results of the measurements are given in Table 10 and 11 and in Figures 22, 23, and 24. It must be noted that the quadrupole S23A:Q4 did not respond to setpoint changes and no data are available for this magnet.

Table 10

	average $\beta_x$ $\overline{\beta_x(m)}$	$\frac{\beta_{x_{max}} - \overline{\beta_x}}{\overline{\beta_x}}$	$\frac{\beta_{x_{min}} - \overline{\beta_x}}{\overline{\beta_x}}$	average $\beta_y$ $\overline{\beta_y(m)}$	$\frac{\beta_{y_{max}} - \overline{\beta_y}}{\overline{\beta_y}}$	$\frac{\beta_{y_{min}} - \overline{\beta_y}}{\overline{\beta_y}}$
individual Q1	16.48	5.2%	-6.6%	7.37	21.0 %	-23.5%
individual Q3	11.22	6.9%	-10.4%	12.14	31.7%	-21.0%
individual Q4	6.47	32.9%	-29.7%	19.18	34.1 %	-28.7%

Table 11

	average $\beta_x$ $\overline{\beta_x(m)}$	average $\beta_y$ $\overline{\beta_y(m)}$
Q1 family	$13.2 \pm 0.59$	$6.58 \pm 0.24$
Q2 family	$21.22 \pm 0.49$	$4.94 \pm 0.26$
Q3 family	$9.60 \pm 0.35$	$10.19 \pm 0.12$
Q4 family	$4.10 \pm 0.86$	$16.05 \pm 0.10$
Q5 family	$11.95 \pm 0.58$	$8.62 \pm 0.32$

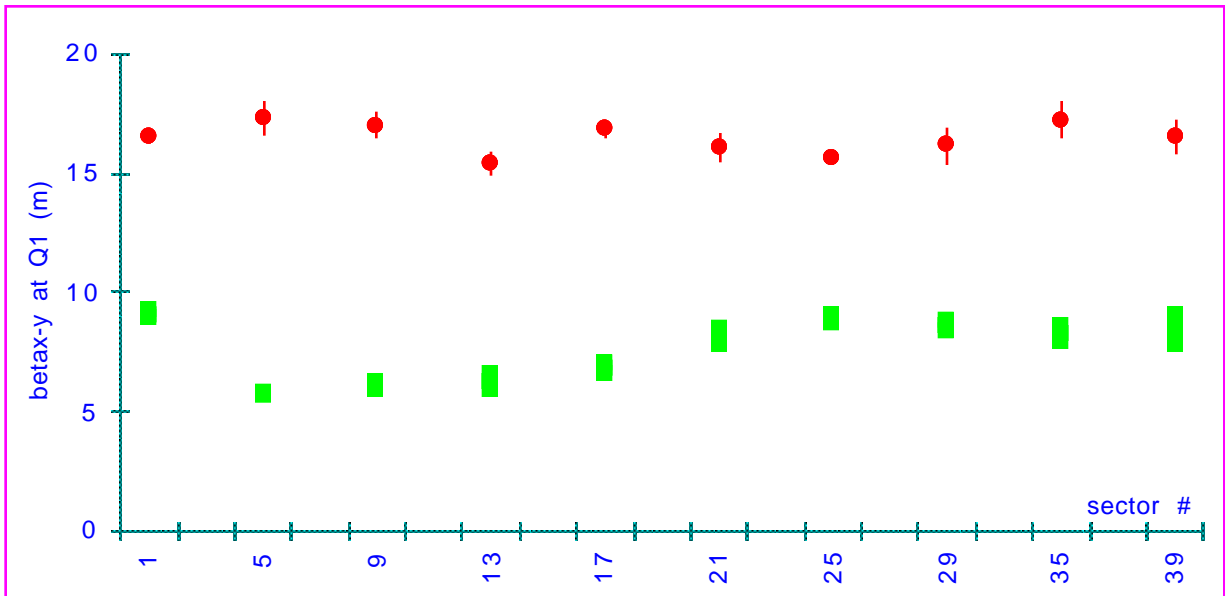


Figure 22.  $\beta$ -function measurements at A:Q1

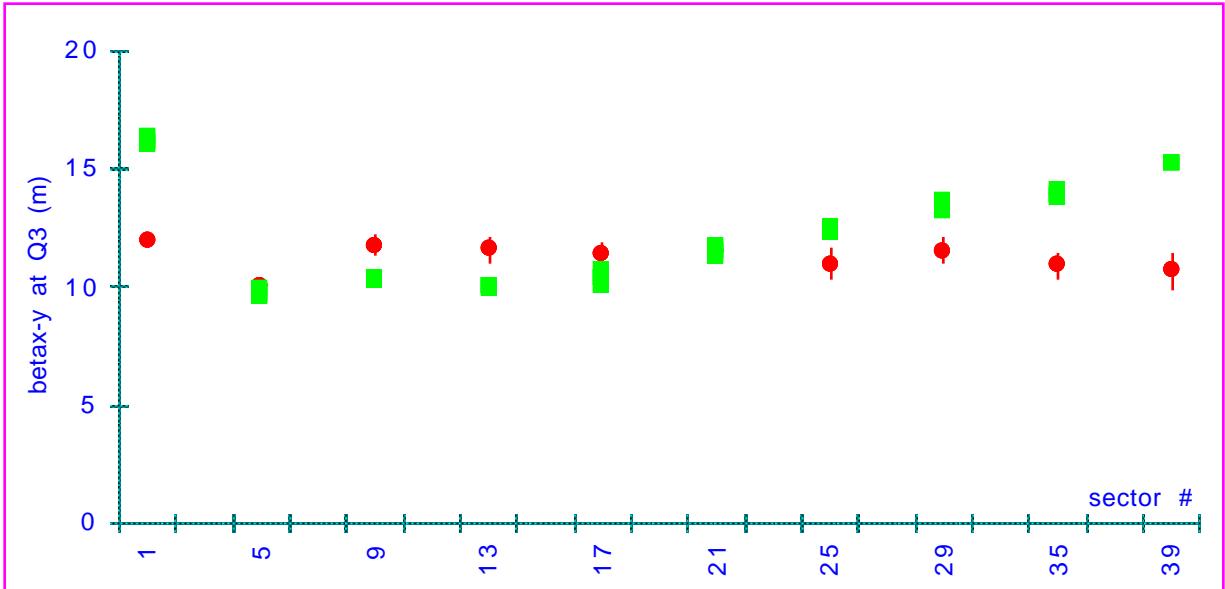


Figure 23.  $\beta$ -function measurements at A:Q3

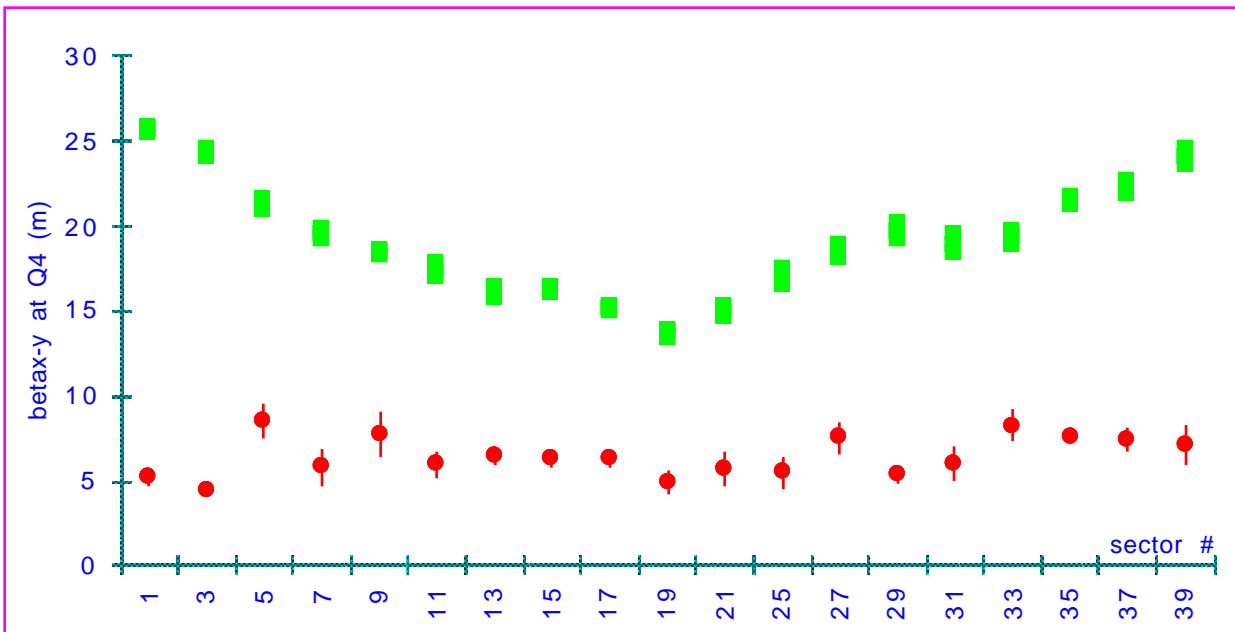


Figure 24.  $\beta$ -function measurements at A:Q4

Several conclusions can be drawn from the processing of the measurements:

- In the horizontal plane, the modulation is less than  $\pm 10\%$ . The error bars for the Q4 measurements are very large due to the combination of small tune shifts and significant jitter on the signals. For comparison, the vertical  $\beta$  at the Q1, which has a similar amplitude, is measured more precisely.

- The modulation in the vertical plane is very large, of the order of  $\pm 30\%$ , and the evolution of  $\beta_y$  at a frequency of twice the vertical tune frequency is clearly seen. The comparative evolution of the modulation in both planes would favour the scenario of a single quadrupole error.

- On the average,  $\beta_y$  stands at much smaller values than the original model or even the revised one with +14 A on Q1 (19 m in the Q4 as opposed to 28 m). It seems that the 14 A change is now overestimated. The reasons for this change and the present evolution are still unclear.

- Average  $\beta$ -functions drawn from the global measurements on quadrupole families are systematically underestimated in both planes, as compared to the average values derived from individual measurements. Whether this results from the simplified processing (which is based on the  $BnL = f(I)$  characteristics of a single quadrupole) or from imprecisions linked to the small  $\Delta I$  applied to each quadrupole of a given family must be investigated.

- Before the S39A:Q4 measurement, the sextupole S6A:S2 tripped. The quadrupole was remeasured after the sextupole was reset. A reproducible  $\beta_y = 19$  m was obtained as opposed to the  $\beta_y = 24$  m measured with the faulty sextupole. If this difference represents the focusing perturbation from one sextupole, it appears difficult to compare the measured  $\beta$ -values to those of a perfect linear model.

The average  $\beta$ -function values (derived from the individual measurements) were used to fit a new model. A very nice convergence was obtained. The new  $\beta$ -functions (dotted lines) are compared to the theoretical ones (plain lines) in Figure 25.

If this new model really represents the machine, it must be pointed out that the vertical  $\beta$  in the straight sections is significantly higher than expected (5 m instead of 3 m). In any case, the fudge factors needed to match the quadrupole currents of the model to the experimental currents now look realistic (see Figure 26) even if the deviations for Q2 and Q3 appear large. Coming back to  $\beta_y = 3$  m in the straight sections would require quadrupole currents very close to the nominal values.

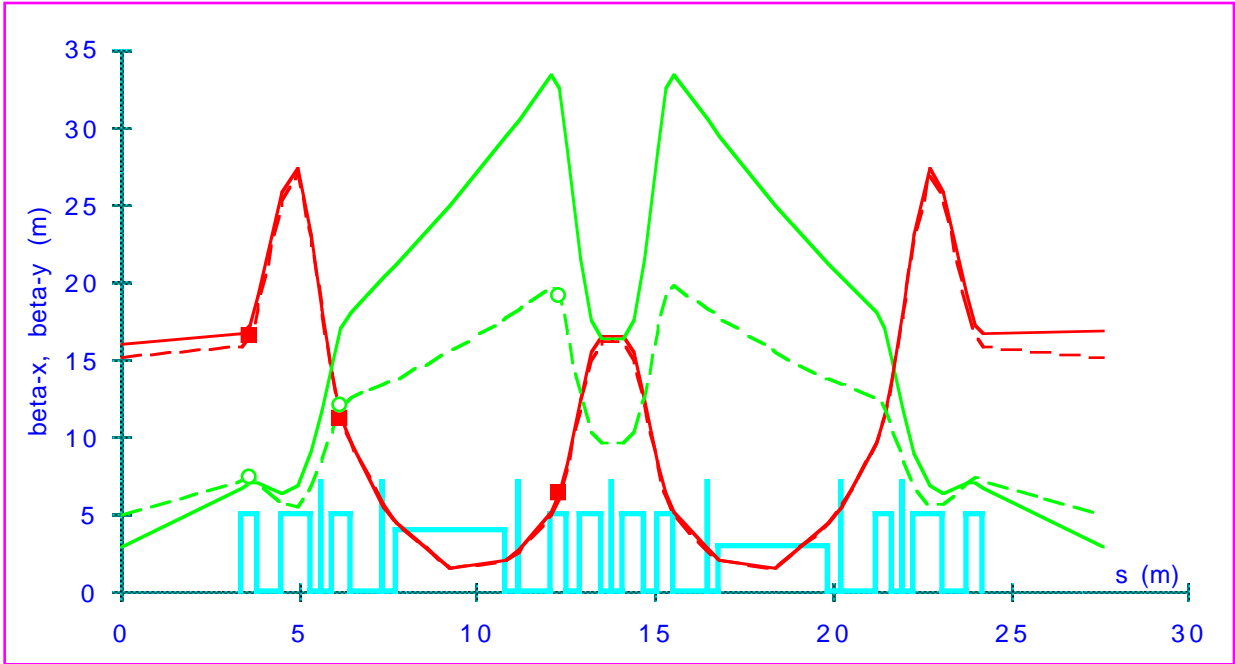


Figure 25. Modeling of the average- $\beta$  function measurements on Mar 30

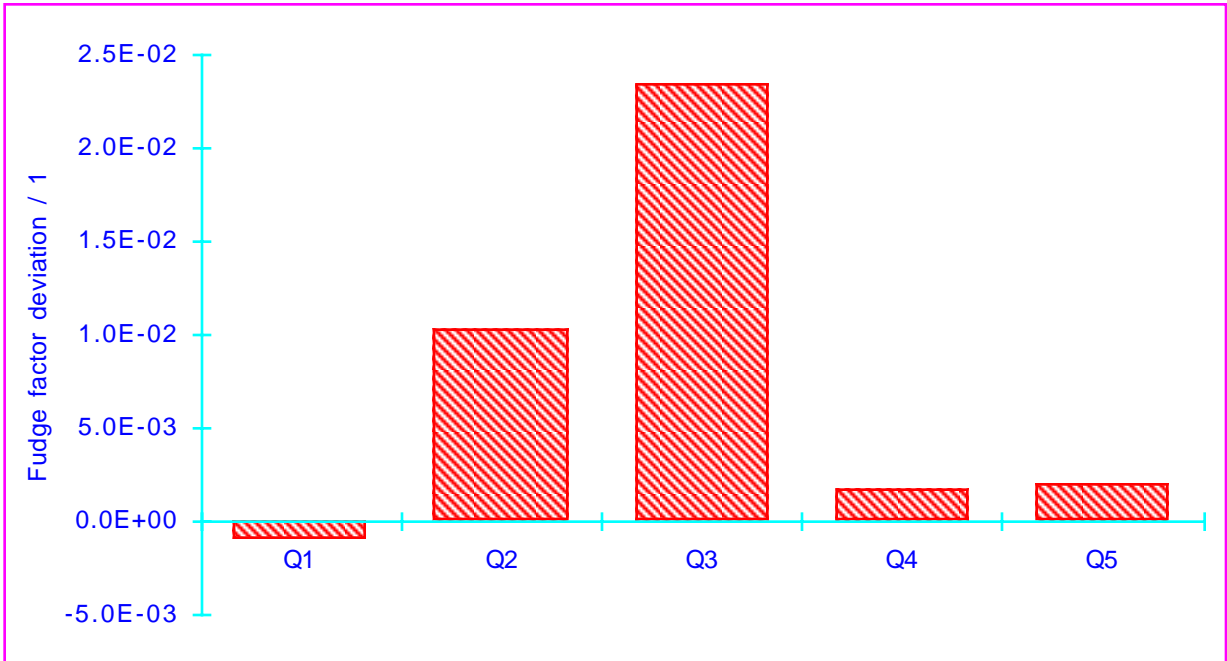


Figure 26. Fudge factors for the new model

Could most of the requested changes in current implemented since the beginning of the run be induced by an insufficient sampling of measured  $\beta$ -functions, given the high modulation, and by the divergence from linear optics linked to the large user orbits in sextupoles? The measurements that were done at the end of the shift after restoring the user orbit (and S20A:S4 to 150 A) leave this second question unanswered. Individual measurements were performed on A:Q4 for half of the machine. As shown in Figure 27, the modulation remains about the same but all  $\beta_y$  values are shifted to lower value than with the centered orbit.

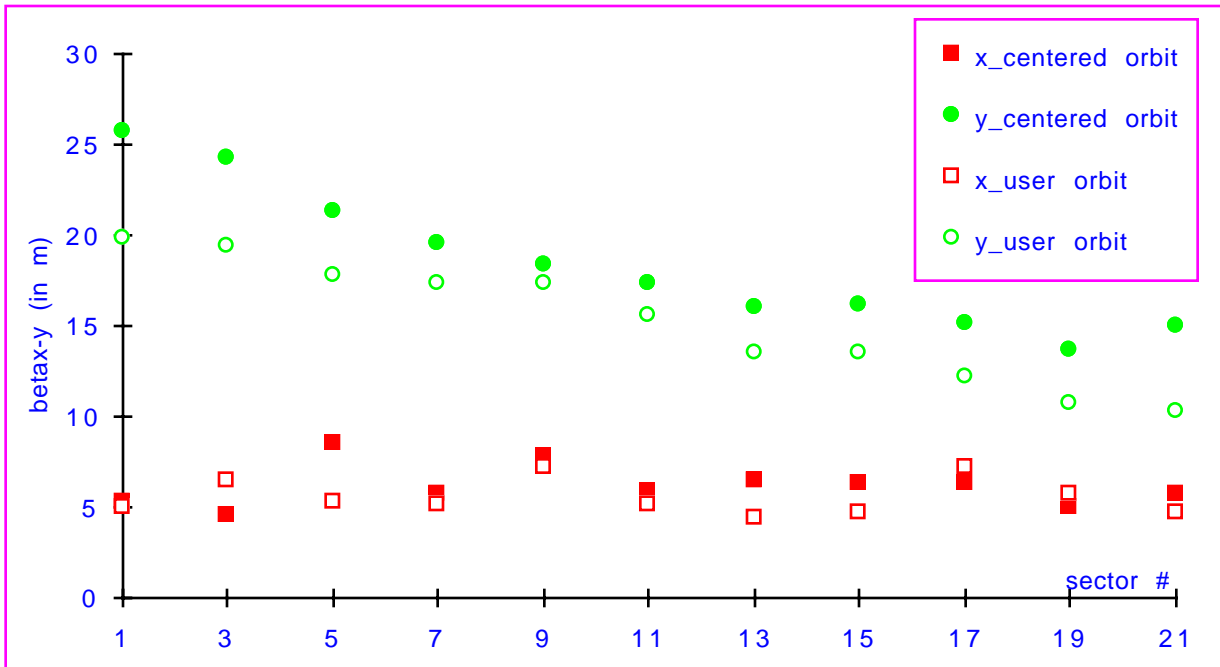


Figure 27. Dependence of measured  $\beta$ -functions on the closed orbit

## Conclusions

The puzzling behaviour of the low  $\beta_y$  optics since the beginning of the run illustrates the fact that a good modeling of the optics is essential. The modeling of the low  $\beta_y$  optics presently relies on the analysis of  $\beta$ -function measurements derived from tune shifts induced by quadrupole current changes. The significant discrepancy between the results of individual and global measurements has to be understood in order to get full confidence in the method.

A number of factors could significantly affect the quality of the modeling:

✍ Although the preliminary observations of the dependence of  $\beta$ -function measurements on the closed orbit have to be confirmed, it looks clear that a good modeling requires minimum

nonlinearities in the machine. The key parameter is therefore the reduction of the closed-orbit distortions.

✍ The measured modulation of the vertical  $\beta$ -function amounts to  $\pm 30\%$  whilst the horizontal one is less than 10%. Given these large variations of  $\beta_y$  along the machine,  $\beta$ -function measurements at a few discrete locations are insufficient and could lead to an over- or underestimation of the real  $\beta$ -functions. This is certainly the source of the irrelevance of the fudge factors derived from the analysis of measurements with several Q1 configurations. This could also partly explain the large change in Q1 applied at the beginning of the run although the recorded evolution of  $\beta$ s with time makes this puzzle even more puzzling.

Attempts were done to identify the origin of the modulation. Since it appears mainly in the vertical plane, the scenario of a single quadrupolar error looks plausible. Scanning the Q4 quadrupoles and measuring the  $\beta$ -functions at another quadrupole should show if this assumption is correct.

The presently proposed model makes use of fudge factors that are different for each quadrupole family and that could reach 2 - 3%. In order to assess their credibility, cross-checks should be done with other optics by measuring a number of  $\beta$ s and comparing the resulting fudge factors to the initial ones.

### **Acknowledgments**

I again would like to thank M. Borland, L. Emery, and N. Sereno for stimulating discussions and for their help during machine studies shifts.